

Supporting Information for

Understanding the dynamic contribution to future changes in tropical precipitation from low-level convergence lines

Evan Weller^{1,2,3}, Christian Jakob^{1,2}, and Michael J. Reeder^{1,2}

¹School of Earth, Atmosphere and Environment, Monash University, Victoria, Australia

²Centre of Excellence for Climate System Science, Monash University, Victoria, Australia

³School of Environment, The University of Auckland, Auckland, New Zealand

Contents of this file

Table S1

Figures S1 to S4

Table S1: CMIP5 models used in this study and their details. The last two columns provide the annual-mean convergence line frequency and strength bias (model minus ERA-Interim) for Historical simulations over the period 1979–2005.

Model	Native resolution (lat × lon)	Modeling center (or group)	Frequency bias (% month ⁻¹)	Strength bias (10 ⁻⁵ s ⁻¹)
ACCESS1.3	1.25 x 1.875	Commonwealth Scientific and Industrial Research Organization (CSIRO) and Bureau of Meteorology (BoM), Australia	-2.7442	-0.0442
BCC-CSM1-1	2.8125 x 2.8125	Beijing Climate Center, China Meteorological Administration	-7.3304	-0.215
BNU-ESM	2.8125 x 2.8125	College of Global Change and Earth System Science, Beijing Normal University	-0.908	-0.0913
CMCC-CM	0.75 x 0.75	Centro Euro-Mediterraneo per I Cambiamenti Climatici, Italy	-1.8036	-0.0817
CNRM-CM5	1.4 x 1.4	Centre National de Recherches Météorologiques/Centre Européen de Recherche et de Formation Avancée en Calcul Scientifique	-4.1073	-0.0221
INM-CM4	1.5 x 2.0	Institute of Numerical Mathematics	-3.7304	-0.0539
MIROC5	1.4 x 1.4	Atmosphere and Ocean Research Institute (University of Tokyo), National Institute for Environmental Studies, & Japan Agency for Marine-Earth Science and Technology, Japan	-1.0551	0.0523
MPI-ESM-MR	1.875 x 1.875	Max Planck Institute for Meteorology, Germany	-4.4726	-0.1111
NCAR-CCSM4	0.9375 x 1.25	National Center for Atmospheric Research, USA	-4.2966	-0.08
NCC-NorESM-M	1.875 x 2.5	Norwegian Climate Centre, Norway	-8.3133	-0.2433

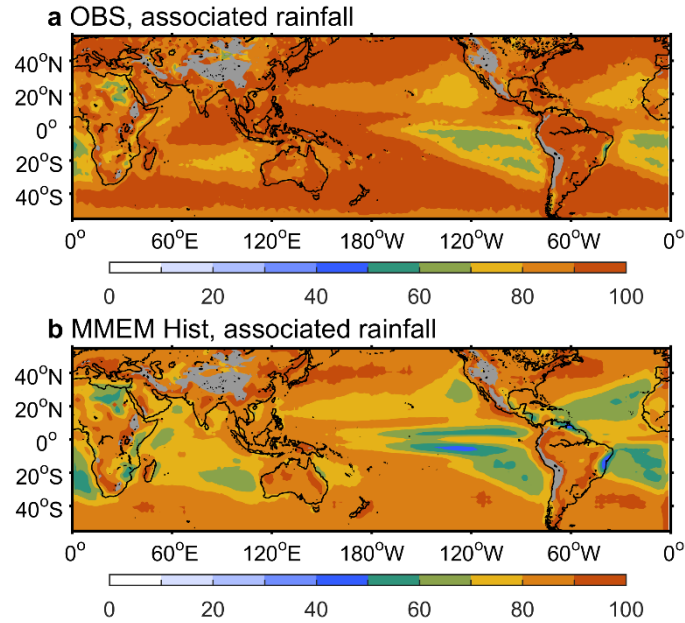


Figure S1 | Amount of observed and modelled historical precipitation associated with convergence lines. a,b, Proportion (in units of %) of the total precipitation from observations and the CMIP5 multi-model ensemble mean (MMEM) the occurs in the presence convergence lines.

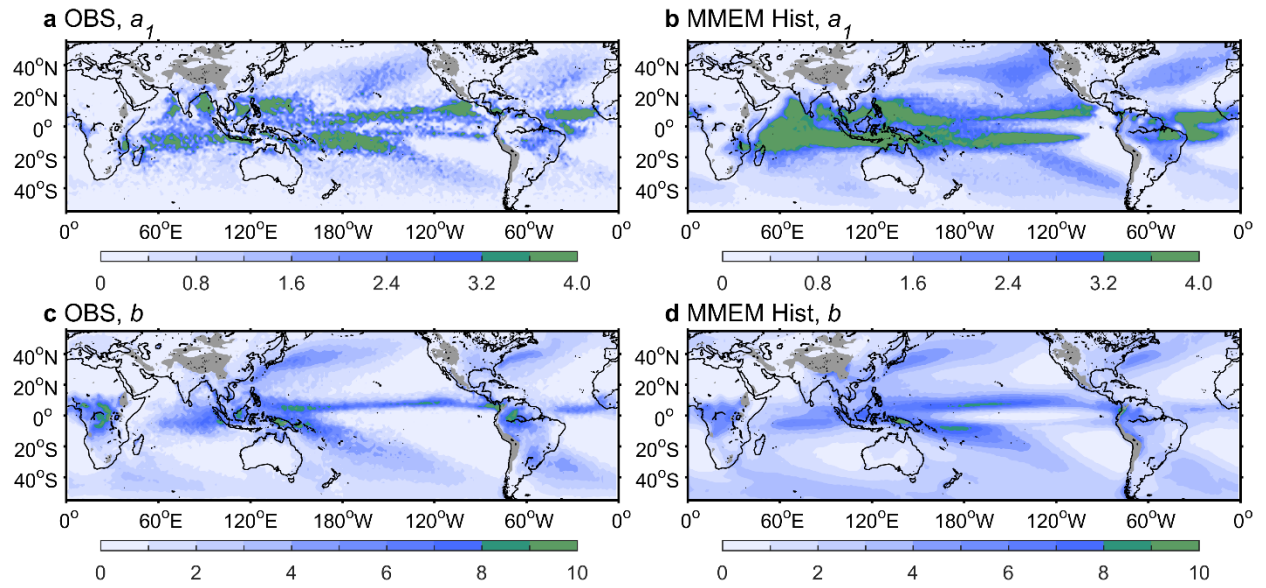


Figure S2 | Linear regression model for reconstructing precipitation. a,b, Observed and multi-model ensemble mean (MMEM) historical regression coefficients (a_1 , in units of mm day^{-1} per 10^{-5} s^{-1}) calculated from the relationship between convergence line strength and precipitation. **c,d,** The same as **a** and **b**, respectively, but for the linear regression intercept (b , in units of mm day^{-1}).

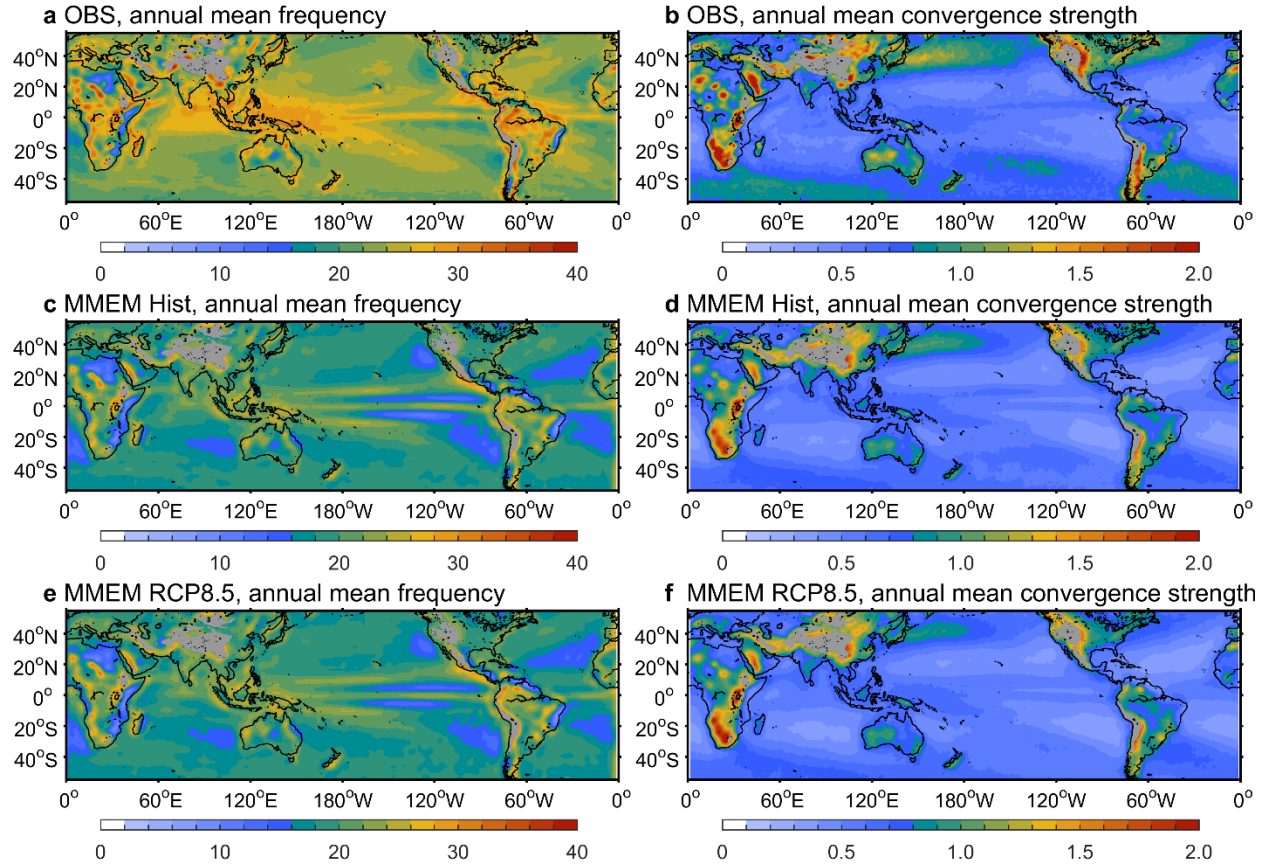


Figure S3 | Historical and future climatological frequency and strength of convergence lines.

a,b, Observed annual mean convergence line frequency (in units of proportion of month ($\% \text{ month}^{-1}$)) and convergence line strength (in units of 10^{-5} s^{-1}). **c,d**, The same as **a** and **b**, respectively, but based on the multi-model ensemble mean (MMEM) historical (1979–2005) simulations. **e,f**, The same as **a** and **b**, respectively, but based on the MMEM RCP8.5 (2080–2100) simulations.

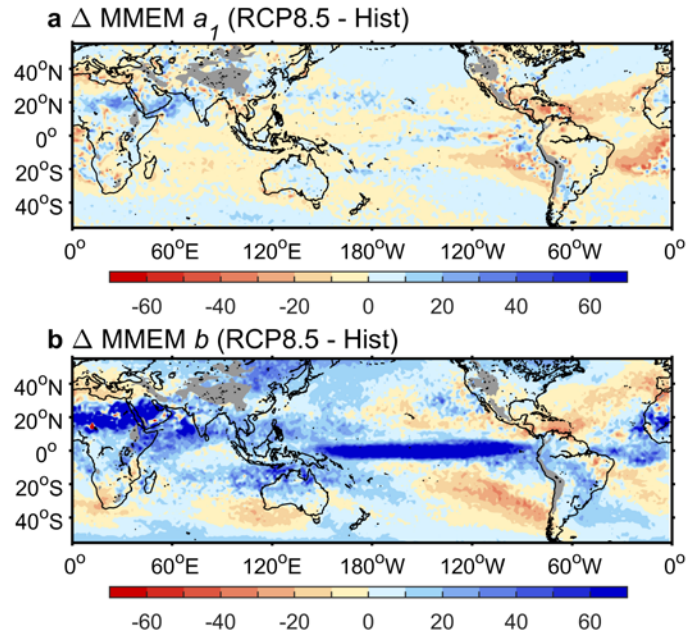


Figure S4 | Future changes in the linear regression model for reconstructing precipitation. a, The CMIP5 multi-model ensemble mean (MMEM) changes (RCP8.5 2080–2100 minus Historical 1979–2005) in the regression coefficient (a_l , in % of the Historical value) calculated from the relationship between convergence line strength and precipitation. **b,** The same as **a** but for the linear regression intercept (b).